

## ORIGINAL ARTICLE

## Control of hepatocyte proliferation and survival by Fgf receptors is essential for liver regeneration in mice

Susagna Padrisa-Altés,<sup>1</sup> Marc Bachofner,<sup>1</sup> Roman L Bogorad,<sup>2</sup> Lea Pohlmeier,<sup>1</sup> Thomas Rossolini,<sup>1</sup> Friederike Böhm,<sup>3</sup> Gerhard Liebisch,<sup>4</sup> Claus Hellerbrand,<sup>5</sup> Victor Koteliansky,<sup>6</sup> Tobias Speicher,<sup>1</sup> Sabine Werner<sup>1</sup>

► Additional material is published online only. To view please visit the journal online (<http://dx.doi.org/10.1136/gutjnl-2014-307874>).

<sup>1</sup>Institute of Molecular Health Sciences, Swiss Federal Institute of Technology (ETH) Zurich, Zurich, Switzerland

<sup>2</sup>David H. Koch Institute for Integrative Cancer Research, Massachusetts Institute of Technology, Cambridge, Massachusetts, USA

<sup>3</sup>Institute of Clinical Pathology, University Hospital of Zurich, Zurich, Switzerland

<sup>4</sup>Department of Clinical Chemistry and Laboratory Medicine, University of Regensburg, Regensburg, Germany

<sup>5</sup>Department of Internal Medicine, University of Regensburg, Regensburg, Germany

<sup>6</sup>Skolkovo Institute of Science and Technology, Skolkovo, Russian Federation

## Correspondence to

Professor Dr Sabine Werner, Institute of Molecular Health Sciences, ETH Zurich, Otto-Stern-Weg 7, 8093, Zurich, Switzerland; [Sabine.werner@biol.ethz.ch](mailto:Sabine.werner@biol.ethz.ch)

Received 18 June 2014

Revised 6 October 2014

Accepted 29 October 2014

Published Online First

21 November 2014



► <http://dx.doi.org/10.1136/gutjnl-2014-307874>



**To cite:** Padrisa-Altés S, Bachofner M, Bogorad RL, et al. *Gut* 2015;**64**:1444–1453.

## ABSTRACT

**Objective** Fibroblast growth factors (Fgfs) are key orchestrators of development, and a role of Fgfs in tissue repair is emerging. Here we studied the consequences of inducible loss of Fgf receptor (Fgfr) 4, the major Fgf receptor (Fgfr) on hepatocytes, alone or in combination with Fgfr1 and Fgfr2, for liver regeneration after PH.

**Design** We used siRNA delivered via nanoparticles combined with liver-specific gene knockout to study Fgfr function in liver regeneration. Liver or blood samples were analysed using histology, immunohistochemistry, real-time RT-PCR, western blotting and ELISA.

**Results** siRNA-mediated knockdown of Fgfr4 severely affected liver regeneration due to impairment of hepatocyte proliferation combined with liver necrosis. Mechanistically, the proliferation defect resulted from inhibition of an Fgf15-Fgfr4-Stat3 signalling pathway, which is required for injury-induced expression of the Foxm1 transcription factor and subsequent cell cycle progression, while elevated levels of intrahepatic toxic bile acids were identified as the likely cause of the necrotic damage. Failure of liver mass restoration in *Fgfr4* knockdown mice was prevented at least in part by compensatory hypertrophy of hepatocytes. Most importantly, our data revealed partially redundant functions of Fgf receptors in the liver, since knockdown of Fgfr4 in mice lacking Fgfr1 and Fgfr2 in hepatocytes caused liver failure after PH due to severe liver necrosis and a defect in regeneration.

**Conclusions** These results demonstrate that Fgf signalling in hepatocytes is essential for liver regeneration and suggest activation of Fgfr signalling as a promising approach for the improvement of the liver's regenerative capacity.

## INTRODUCTION

Fibroblast growth factors (Fgfs) comprise a family of 22 proteins in mammals, which control proliferation, differentiation and survival of various cell types. They exert their functions by activation of four transmembrane tyrosine kinase receptors, designated Fgfr1–Fgfr4.<sup>1–2</sup> Fgf expression is strongly upregulated after injury to various tissues and organs as initially demonstrated for the skin.<sup>3</sup> This is functionally important since inhibition of Fgfr signalling in mice caused impaired wound healing<sup>4</sup> and also affected the repair process of other organs.<sup>2,5</sup> Therefore, Fgfs

## Significance of this study

## What is already known on this subject?

- Fibroblast growth factor receptor (Fgfr)1 and Fgfr2 on hepatocytes control compound detoxification in the regenerating liver.
- Global loss of Fgfr4 in mice does not cause an obvious defect in liver regeneration after partial hepatectomy.
- Loss of Fgf15, the major Fgfr4 ligand, strongly impairs hepatocyte proliferation and causes liver damage after partial hepatectomy.

## What are the new findings?

- Inducible loss of Fgfr4 in the liver through siRNA-mediated knockdown severely impairs liver regeneration.
- Fgf15 levels increase in the serum after partial hepatectomy and most likely activate Fgfr4 on hepatocytes.
- Mechanistic studies reveal that an Fgf15-Fgfr4-Stat3-FoxM1 axis controls hepatocyte proliferation in the regenerating liver.
- Combined loss of Fgfr1, Fgfr2 and Fgfr4 in hepatocytes causes liver failure after partial hepatectomy, demonstrating that Fgfr signalling is essential for liver regeneration.

## How might it impact on clinical practice in the foreseeable future?

- Activation of Fgfr4 signalling through treatment with the ligand Fgf15 or low-molecular-weight compounds is a promising approach for the improvement of liver regeneration, in particular in patients with severe liver damage.

are promising molecules for the treatment of impaired tissue repair.

The liver is the only organ in adult mammals that can fully regenerate even after severe injury.<sup>6–7</sup> This remarkable regenerative capacity involves the action of different growth factors, and ligands of the epidermal growth factor receptor as well as hepatocyte growth factor (Hgf) are considered as the major mitogens for hepatocytes in the regenerating liver.<sup>7,8</sup> Our previous studies also revealed a

role of Fgfs in this process since hepatocyte proliferation after two-third (partial) hepatectomy (PH) was impaired in mice expressing a dominant-negative Fgfr2 mutant in hepatocytes.<sup>9</sup> Since this mutant inhibits signalling via different Fgfr to a different extent, the role of individual receptors in the regenerative response and their mechanisms of action remained, however, unclear. Therefore, we studied the liver regeneration process in mice lacking Fgfr1 and Fgfr2 in hepatocytes and identified an important function of these receptors in compound detoxification, while the peak in hepatocyte proliferation was only mildly affected.<sup>10</sup> By contrast, no obvious regeneration defect after PH was observed in mice with a global *Fgfr4* knockout,<sup>11</sup> although Fgfr4 is the most abundant Fgfr on hepatocytes with an important function in liver tumorigenesis.<sup>12–13</sup> Since mice with a global knockout of a gene frequently activate compensatory pathways during prenatal and/or postnatal development, we studied the consequences of an inducible loss of this receptor in adult mice for liver regeneration. We used siRNA formulated into lipid nanoparticles, which allows an efficient knockdown in the liver after a single injection.<sup>14</sup> The nanoparticles specifically target hepatocytes due to an apolipoprotein E-dependent mechanism of delivery.<sup>15–17</sup> Recently, we demonstrated the usefulness of an siRNA approach to determine the role of  $\beta$ 1-integrin in liver regeneration.<sup>18</sup> Importantly, the knockdown was only efficient in hepatocytes, but not in non-parenchymal liver cells.<sup>18</sup> Using this approach, we determined the consequences of Fgfr4 knockdown for liver regeneration in the presence or absence of Fgfr1 and Fgfr2 in hepatocytes. We demonstrate an important role of Fgfr4 in liver regeneration and an essential role of Fgfr signalling in general for this process.

## MATERIALS AND METHODS

### Animals

Wild-type mice, mice lacking Fgfr1 and Fgfr2 in hepatocytes<sup>10</sup> and mice expressing Cre recombinase in hepatocytes (Alb-Cre mice) were used in this study. They were maintained in a pathogen-free facility under optimal hygiene conditions. Mouse maintenance and all procedures with animals had been approved by the local veterinary authorities of Zurich, Switzerland.

### siRNA-mediated knockdown

siRNAs were formulated in lipid nanoparticles (ionisable lipids), which specifically target hepatocytes due to an apolipoprotein E-dependent mechanism of delivery.<sup>15–17</sup> Male mice received formulated siRNA directed against luciferase (*Luc*) or Fgfr4 (0.5 mg/kg) via tail vein injection in a volume of 5 mL/kg body weight at days 1 and 5. PH was performed at day 10. The following siRNAs were used:

Fgfr4	Sense 5'-ccuGAuGcAucGAcAuuuAdTsdT-3'
	Antisense 5'-uAAAUGUCGAUGcAUCAGGdTsdT-3'
Fgfr4-2	Sense 5'-GGcuGAAAcAcGucGucAudTsdT-3'
	Antisense 5'-AUGACGACGUGUUCAGCCdTsdT-3'
Luciferase	Sense 5'-cuuAcGcuGAGuAcuucGAdTsdT-3'
	Antisense 5'-UCGAAGuACuACGGuAAGdTsdT-3'

2'-OMe modified nucleotides are in lower case, and phosphorothioate linkages are indicated by 's'.

### Partial hepatectomy

Eight-week to 10-week-old male mice, which had received food and water ad libitum before surgery, were anaesthetised

by inhalation of isoflurane, and PH was performed in the morning between 08:00 and 12:00.<sup>10</sup> After PH, mice were injected with buprenorphine for analgesia (Temgesic; Essex Chemie AG, Luzern, Switzerland; 0.1 mg/kg of body weight). They were euthanised by CO<sub>2</sub> inhalation, and the remaining liver was removed at different time points after PH. The liver tissue that was removed during PH was considered 0 h time point.

### Histology and histomorphometry

Liver samples were fixed in 4% paraformaldehyde in phosphate buffered saline (PBS) or in 95% ethanol/1% acetic acid and embedded in paraffin. Sections (3.5  $\mu$ m) were stained with H&E and photographed. The necrotic area was determined morphometrically. For cell size measurement, acidic ethanol-fixed sections were permeabilised with Triton X-100 and the actin cytoskeleton was stained with rhodamine-coupled phalloidin (Life Technologies, Carlsbad, California, USA). Nuclei were counterstained with 4',6-diamidino-2-phenylindole. Sections were mounted with Mowiol.

### Identification of proliferating cells in vivo

Proliferating cells were identified by 5-bromo-2'-deoxyuridine (BrdU) labelling 2 h before sacrifice. Liver sections were stained with a BrdU antibody, and labelled cells were counted in four independent microscopic fields (200 $\times$  magnification) per animal.<sup>10</sup>

### Isolation of parenchymal and non-parenchymal cells from mouse liver

Liver was perfused and digested, and hepatocytes and non-parenchymal cells were separated as described.<sup>19</sup>

### Terminal dUTP nick-end labelling

The *In Situ Cell Death Detection Kit* (Roche, Basel, Switzerland) was used for the detection of apoptotic cells.

### Serum analysis

After sacrifice, blood was taken by heart punctation. After coagulation, serum was harvested, snap-frozen and analysed using FUJI DRI-CHEM 4000i and the corresponding reagents (Fuji, Tokyo, Japan).

### Immunohistochemistry

Paraffin sections were incubated for 30 min in 12% bovine serum albumin in PBS/0.025% NP-40 to block unspecific binding sites. The primary antibody (anti-Ly6G; BD Pharmingen, Allschwil, Switzerland) was incubated overnight at 4°C. Sections were stained using the ABC Vectastain Peroxidase Kit (Vector Laboratories, Burlingame, California, USA) according to the manufacturer's protocol, counterstained with haematoxylin, rehydrated and mounted.

### RNA isolation and quantitative RT-PCR analysis

Isolation of total cellular RNA, cDNA synthesis and quantitative RT-PCR (qRT-PCR) were carried out as described previously<sup>10</sup> using the following primers:

Gapdh	Forward: 5'-TCG TGG ATC TGA CGT GCC GCC TG-3' Reverse: 5'-CAC CAC CCT GTT GCT GTA GCC GTA T-3'
Fgfr4	Forward: 5'-TTG GCC CTG TTG AGC ATC TTT-3' Reverse: 3'-GCC CTC TTT GTA CCA GTG ACG-3'
Fgfr1	Forward: 5'-CAA CCG TGT GAC CAA AGT GG-3' Reverse: 5'-TCC GAC AGG TCC TTC TCC G-3'

## Hepatology

Fgfr2	Forward: 5'-ATC CCC CTG CGG AGA CA-3' Reverse: 5'-GAG GAC AGA CGC GTT GTT ATC C-3'
Fgfr3	Forward: 5'-GTG GCT GGA GCT ACT TCC GA-3' Reverse: 5'-ATC CTT AGC CCA GAC CGT GG-3'
Foxm1	Forward: 5'-TGA CAT TGG ACC AAG TGT TTA AGC-3' Reverse: 5'-TCG TTT CTG CTG TGA TTACCA GT-3'
Cyclin D1	Forward: 5'-GCG TAC CCT GAC ACC AAT CTC-3' Reverse: 5'-ACT TGA AGT AAG ATA CGG AGG GC-3'
Cyclin E1	Forward: 5'-TCC ACG CAT GCT GAA TTA TC-3' Reverse: 5'-TTG CAA GAC CCA GAT GAA GA-3'
Cyclin A2	Forward: 5'-CTT GGC TGC ACC AAC AGT AA-3' Reverse: 5'-CAA ACT CAG TTC TCC CAA AAA CA-3'
Cyclin B1	Forward: 5'-GCG TGT GCC TGT GAC AGT TA-3' Reverse: 5'-CCT AGC GTT TTT GCT TCC CTT-3'
Cyp7a1	Forward: 5'-GGG ATT GCT GTG GTA GTG AGC-3' Reverse: 5'-CTG TTG CCC AAC TAA GGT ATG G-3'
Fxr	Forward: 5'-GCTTGATGTGCTACAAAGCTG-3' Reverse: 5'-CGTGGTGATGGTTGAATGTC-5'
Tbp	Forward: 5'-AGA ACA ATC CAG ACT AGC AGC A-3' Reverse: 5'-GCC CTC TTT GTA CCA GTG ACG-3'

### Cell culture

Mouse immortalised hepatocytes (AML12 cells), Hepa1-6 hepatoma cells and C2C12 myoblasts were cultured in DMEM/10% FCS/penicillin/streptomycin.

### Preparation of protein lysates and western blot analysis

Frozen tissue was homogenised in T-PER tissue protein extraction reagent (Pierce, Rockford, Illinois, USA) containing Complete Protease Inhibitor Cocktail and PhosSTOP Phosphatase Inhibitor Cocktail (Roche). Lysates were cleared by sonication and centrifugation.

Cultured cells were lysed in 1× Laemmli buffer at 95°C. Proteins were analysed by western blotting using antibodies against Fgfr4 (R&D Systems, Minneapolis, Minnesota, USA), Gapdh (HyTest, Turku, Finland), Foxm1 and Cyp7a1 (Santa Cruz, Santa Cruz, California, USA), phospho-STAT3 (Tyr-705) and total-STAT3 (both from Cell Signaling, Beverly, Massachusetts, USA).

### Cell cycle analysis of cultured cells

Incorporation of 5-ethynyl-2'-deoxyuridine (EdU) into DNA was monitored by flow cytometry using the Click-iT EdU Flow Cytometry Assay kit (Invitrogen, Basel, Switzerland). The same staining provided information on the cell cycle state of the cells. Hepa1-6 cells were cultured in 6-well plates and transfected with *Luc* or *Fgfr4* siRNA (10 nM siRNA) using lipofectamine (Sigma, Buchs, Switzerland). After 48 h incubation, EdU was added to a final concentration of 10 µM. Four hours later, cells were removed by 5 min accutase treatment (1:10, Lucerna-Chem, Luzern, Switzerland). Cells were analysed using a BD LSRII Fortessa (BD, Allschwil, Switzerland) and FlowJo V8.7 software (Treestar, Ashland, Oregon, USA).

### Determination of Fgf15 serum levels

Serum levels of Fgf15 were determined by ELISA (Antibodies-online.com, Aachen, Germany) according to the manufacturer's instructions.

### Cytokine multiplex ELISA

Cytokine concentrations were measured in 50 µg liver lysate using the magnetic bead multiplex suspension array system (Bio-Plex ProT Mouse Cytokine 23-plex Assay; BioRad; Hercules, California, USA). Data were analysed using the MagPix instrument and Bioplex Software (BioRad).

### Bile acid quantification

Bile acids were quantified by liquid chromatography-tandem mass spectrometry (LC-MS/MS).<sup>20</sup> Instead of serum, liver homogenates corresponding to 1.25 mg wet weight were analysed.

### Statistical analysis

Statistical analysis was performed using the Prism6 software (GraphPad Software, San Diego, California, USA). Quantitative data are expressed as mean±SEM. Significance was calculated using Mann-Whitney U test; \*p≤0.05, \*\*p≤0.01, \*\*\*p≤0.001.

## RESULTS

### Impaired liver regeneration after siRNA-mediated knockdown of Fgfr4

We used lipid-based nanoparticles to deliver *Fgfr4* siRNA to hepatocytes. Forty-four *Fgfr4* siRNAs were tested for their in vitro efficacy using C2C12 mouse myoblasts, which express high levels of Fgfr4. The most potent siRNAs—*Fgfr4* and *Fgfr4-2* (see online supplementary figure S1A)—were packaged into nanoparticles. siRNA against *Luc* was used as control. Nanoparticles were injected into the tail vein at day 1 and day 5, and mice were subjected to PH 5 days later (figure 1A). The initial analysis of non-injured liver and liver 48 h after PH was performed with wild-type and Alb-Cre mice, and the results were identical (data not shown). Since it was the ultimate goal to knock down Fgfr4 in mice lacking Fgfr1 and Fgfr2 in hepatocytes (Alb-R1/R2 mice<sup>10</sup>), Alb-Cre mice were used for all follow-up studies since they are the appropriate control for Alb-R1/R2 mice.

Efficient knockdown of Fgfr4 was verified by qRT-PCR using RNAs from total liver or cultured primary hepatocytes and by western blotting using total liver lysates (figure 1B). The similar knockdown efficiency seen with lysates from total liver and from isolated hepatocytes is consistent with the strong expression of Fgfr4 by hepatocytes, but not by non-parenchymal cells (see online supplementary figure S1B). Efficient knockdown by *Fgfr4* siRNA was confirmed for all time points and by *Fgfr4-2* siRNA for the 48 h time point, while expression of other Fgfr was not affected (see online supplementary figure S1C–E). Knockdown of Fgfr4 did not cause liver injury within the analysed time frame as revealed by normal serum levels of aspartate and alanine aminotransferases (AST and ALT) (figure 1C) and the normal liver histology (see online supplementary figure S1F). Most control mice survived the first week after PH, whereas 25% of the mice with Fgfr4 knockdown died between 48 and 216 h after surgery (see online supplementary figure S2A). ALT and AST levels were increased compared with control mice at 24 and 48 h after PH (figure 1C). Severe necrosis was observed up to 48 h, in particular around portal areas (figure 1D), and there was enhanced steatosis, neutrophil infiltration and an increase in the number of apoptotic cells (see online supplementary figure S2B–D). Their small nuclei suggest that the apoptotic cells are predominantly non-parenchymal cells. The damage was, however, repaired during the following days (figure 1D). The peak in hepatocyte DNA replication that occurred in control mice at 48 h after PH was not observed after Fgfr4 knockdown. There was no compensatory hyperproliferation at later time points (figure 1E) and also no increase compared with control at 36 h (data not shown). Since we still observed a strong knockdown after 9 days (see online supplementary figure S1C), it is unlikely that cells with inefficient knockdown preferentially contributed to regeneration.

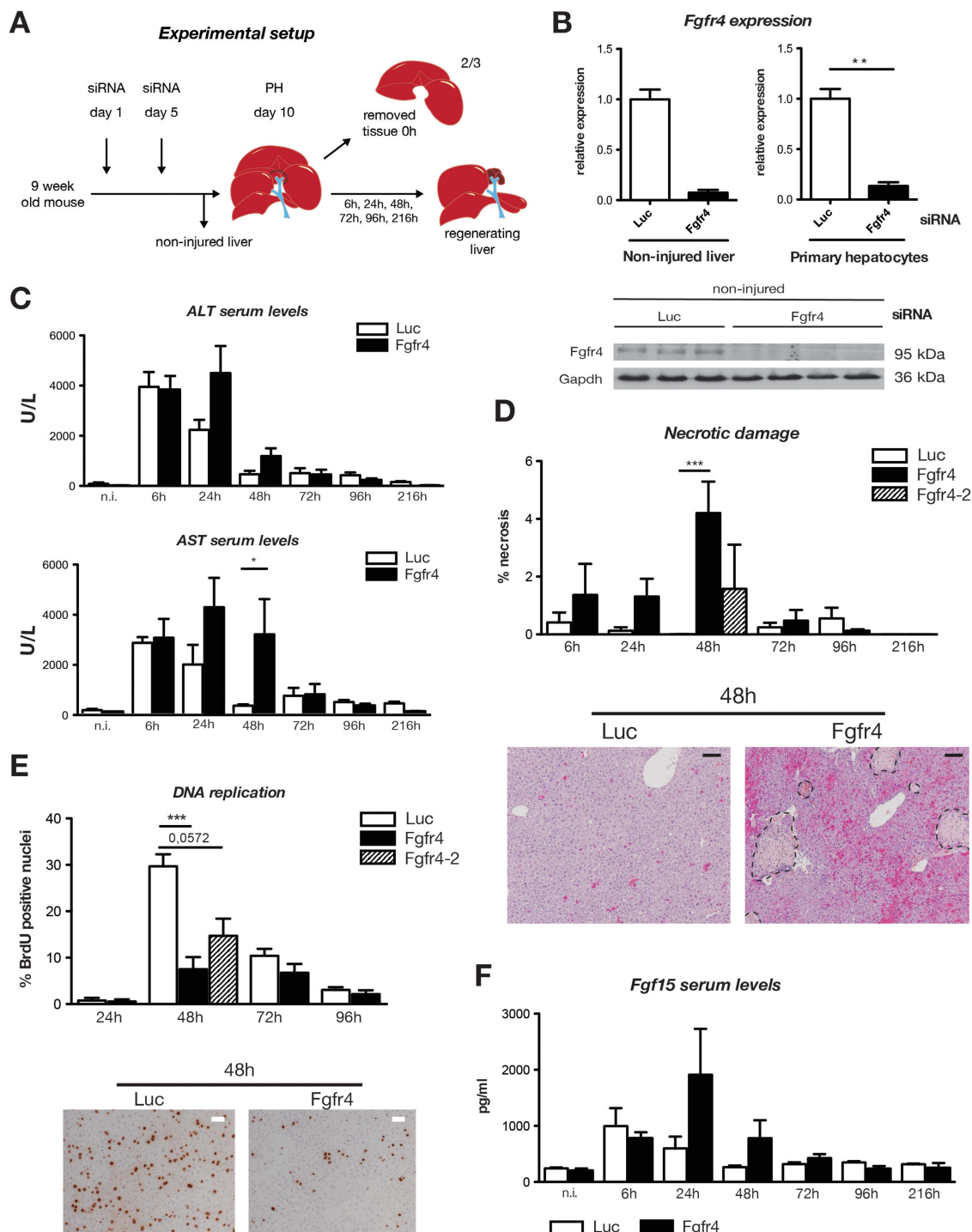


**Figure 1** Impaired liver regeneration in mice after knockdown of Fgfr4 in hepatocytes. (A) Schematic representation of the experimental setup. Mice were injected twice with *Fgfr4* or *Luc* siRNA with a time interval of 5 days. After additional 5 days, they were subjected to two-third (partial) hepatectomy (PH). (B) Knockdown of Fgfr4 was verified by qRT-PCR using RNA from total liver or cultured primary hepatocytes. N=3–7 per treatment group. Expression levels in mice treated with *Luc* siRNA were arbitrarily set as 1. (C) Activities of ALT and AST in the serum were determined in non-injured mice (n.i.) and at different time points after PH (N=3–9). (D) Morphometric analysis of the necrotic damage using H&E-stained liver sections at different time points after PH in mice injected with *Fgfr4* siRNA and at 48 h in mice injected with *Fgfr4-2* siRNA. N=4–9. Representative sections from mice 48 h after PH are shown below. Necrotic areas are encircled with dotted lines. Scale bar: 100  $\mu$ m. (E) BrdU-positive cells were counted in liver sections at different time points after PH in mice injected with *Fgfr4* siRNA and at 48 h in mice injected with *Fgfr4-2* siRNA. N=4–9. Representative sections stained with a BrdU antibody are shown for the 48 h time point. Scale bar: 50  $\mu$ m. (F) Levels of Fgf15 in the serum were determined in non-injected mice and at different time points after PH. N=3–5. All bars represent mean  $\pm$  SEM. ALT, alanine transaminase; AST, aspartate transaminase; BrdU, 5-bromo-2'-deoxyuridine; Fgfr, fibroblast growth factor receptor; Luc, luciferase.

Similar regeneration defects were observed with *Fgfr4-2* siRNA (figure 1D, E), and the more efficient siRNA (*Fgfr4*) (see online supplementary figure S1A) caused a stronger phenotype

compared with the less efficient siRNA (*Fgfr4-2*). Mice injected with *Luc* siRNA did not exhibit necrosis (figure 1D), and the time course of regeneration as well as AST/ALT levels after PH



**Table 1** Enhanced levels of bile acids in mice with *Fgfr4* knockdown

Bile acid SPECIES	n.i.		24 h		48 h		72 h	
	Luc	<i>Fgfr4</i>	Luc	<i>Fgfr4</i>	Luc	<i>Fgfr4</i>	Luc	<i>Fgfr4</i>
Total	243.5±58.9	194±33.8	538.2±427.9	2486.2±1424.1	183.3±36.3	1508.1±656*	331.8±84.1	430.4±171.2
Free	0.1±0.1	0±0	1±1	33.5±24.6	0±0	3.8±2.4	0±0	1.4±1.3
Primary	215.4±54.4	172.9±32.9	524.6±428	2432±1389.9	168.3±34.4	1493.9±658.9	321.3±84	420.6±171.7
Secondary	28.1±4.6	21.1±5.9	13.6±2.3	54.2±36	15.1±3.3	14.2±3	10.4±3.3	9.8±0.8
Tauro	243.3±58.9	194±33.8	537.2±426.9	2452.7±1399.7	183.3±36.3	1504.3±653.7*	331.7±84.1	429±170.3
FREE								
Primary								
CA	0.1±0.1	0±0	1±1	32.3±23.6	0±0	3.8±2.4	0±0	1.4±1.3
Secondary								
HDCA	0±0	0±0	0±0	0.9±0.7	0±0	0±0	0±0	0±0
DCA	0±0	0±0	0±0	0.2±0.2	0±0	0±0	0±0	0±0
LCA	0±0	0±0	0±0	0±0	0±0	0±0	0±0	0±0
TAURO-CONJUGATED								
Primary								
TCA	203.4±53	166.8±31.6	517.4±425.2	2393.1±1363.8	158.3±34.1	1474.4±657.9*	303.3±82.8	399.6±172.1
TCDCa	11.8±2.5	6.1±1.3	6.2±1.7	6.6±2.8	9.9±0.8	15.7±1.4*	18±5.5	19.5±2.1
Secondary								
TUDCA	18.5±2.3	10.5±4.2	5.3±1.3	24±18.4	6.5±1.4	7.2±1.4	4.1±1.5	7.3±1.6
THDCA	3±1.3	3±0.7	3.7±0.8	12.7±9.5	4.9±1.6	4.2±0.7	3.8±1.3	0.8±0.3
TDCA	6.6±1.7	7.6±1.4	4.6±2.9	16.3±7.6	3.7±1	3.5±1	2.5±1.3	2.5±0.7

Levels of individual intrahepatic bile acids were determined prior to and at different time points after PH using liquid chromatography—mass spectrometry and are shown as nanomole bile acid per gram liver tissue. Values indicate mean±SEM. Bile acids, which were significantly higher in mice with *Fgfr4* knockdown compared with mice injected with *Luc* siRNA are indicated with \*.

CA, cholic acid; DCA, deoxycholic acid; *Fgfr*, fibroblast growth factor receptor; HDCA, hyodeoxycholic acid; LCA, lithocholic acid; Luc, luciferase; n.i., non-injured mice; PH, partial hepatectomy; TCA, taurocholic acid; TCDCa, taurochenodeoxycholic acid; TDCA, taurodeoxycholic acid; THDCA, taurohyodeoxycholic; TUDCA, tauroursodeoxycholic acid.

were similar as in mice not injected with any siRNA<sup>18</sup> (and data not shown). This finding demonstrates lack of toxicity of the nanoparticles even after liver injury.

Levels of the major *Fgfr4* ligand, *Fgf15*,<sup>21</sup> strongly increased in the serum of control mice within 6–24 h after PH, most likely as a result of release of intrahepatic bile acids into the intestine after surgery. This increase was much more pronounced after *Fgfr4* knockdown (figure 1F), possibly due to higher levels of bile acids that stimulate *Fgf15* expression in the intestine,<sup>21</sup> since activation of *Fgfr4* by intestinal *Fgf15* suppresses bile acid production.<sup>11</sup> Indeed, expression of cholesterol 7  $\alpha$ -hydroxylase (*Cyp7a1*), the rate-limiting enzyme in bile acid production,<sup>22</sup> was increased in mice with *Fgfr4* knockdown prior to PH (see online supplementary figure S3A), and the concentrations of intrahepatic bile acids, in particular of tauro-conjugated bile acids, were significantly higher than in control mice at 24 and 48 h after PH (table 1 and see online supplementary figure S3B). The increase in bile acids in the liver during regeneration provides an explanation for the liver necrosis since bile acids can damage cell membranes due to their detergent properties.<sup>23</sup> The necrosis is most likely not due to increased fragility of bile ductules in the absence of *Fgfr4* since staining with a pan-keratin antibody revealed no obvious defect in the integrity of bile ducts at periportal locations (see online supplementary figure S3C).

### Loss of *Fgfr4* induces compensatory hepatocyte growth

In spite of the defect in DNA replication by hepatocytes, the liver to body weight ratio was only mildly reduced in the *Fgfr4* knockdown mice 96 and 216 h after PH (figure 2A), suggesting that cellular hypertrophy compensates at least in part for the proliferation defect. Indeed, hepatocytes of these mice were

significantly larger at 216 h after PH compared with control mice, and more cells were binuclear at this time point (figure 2B, C). There was also a strong reduction in mitotic figures 48 h after PH. However, this was followed by an increase at 72 h (figure 2D), demonstrating that cell division eventually occurred, although with a severe delay.

### *Fgfr4* signalling is important for Stat3 activation and PH-induced expression of the forkhead box protein M1 (*Foxm1*)

Consistent with the defect in cell cycle progression upon *Fgfr4* knockdown, expression of cyclins A2 and B1 was reduced at 48 h after PH compared with *Luc* siRNA injected mice, while cyclins D1 and E1 were only moderately affected (figure 3A–D). Upregulation of *Foxm1*, a transcription factor with a crucial role in hepatocyte DNA replication and mitosis after PH,<sup>24</sup> occurred 48 h after PH in control mice, but to a much lesser extent in *Fgfr4* knockdown mice (figure 3E). This was not due to alterations in the expression of the farnesoid X receptor (*Fxr*), a direct activator of the *Foxm1* gene (figure 3F). However, levels of phosphorylated (activated) Stat3, a positive regulator of the *Foxm1* gene,<sup>25</sup> were much lower in *Fgfr4* knockdown mice at 24 h after PH compared with controls, while the early Stat3 activation was not affected (figure 3G). This was not a consequence of interleukin (IL)-6 deficiency since serum levels of IL-6 and its upstream regulator tumour necrosis factor- $\alpha$  were even increased in mice with *Fgfr4* knockdown at this time point (see online supplementary figure S4A,B). Rather, it seems to be a direct consequence of the reduction in *Fgfr4* levels since *Fgfr4* knockdown in mouse hepatoma cells also reduced Stat3 phosphorylation. Concomitantly, DNA synthesis was reduced and cells in G1 accumulated, whereas those in S or G2 phase were

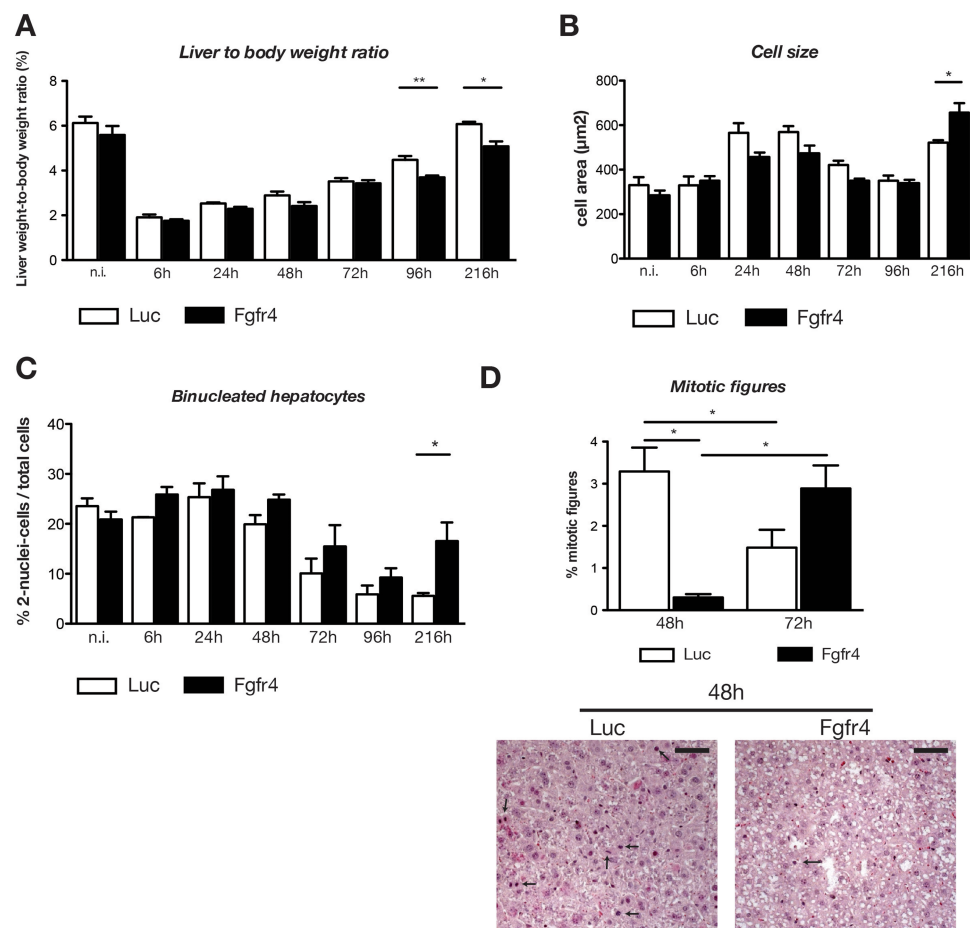


**Figure 2** Compensatory growth of hepatocytes after PH in mice with *Fgfr4* knockdown. (A) Liver to body weight ratio in non-injured mice and at different time points after PH in mice injected with *Fgfr4* or *Luc* siRNA. N=3–9 mice per treatment group. (B) Size of hepatocytes as determined on sections stained with rhodamine-coupled phalloidin. (C) The percentage of binucleated cells was determined on sections stained with rhodamine-coupled phalloidin. (D) Cells with mitotic figures (indicated by arrows in the representative stainings) were quantified in H&E-stained sections. Approximately 50 cells from three to seven mice were counted in (B–D). Magnification bar: 50 μm. Bars represent mean±SEM. *Fgfr*, fibroblast growth factor receptor; *Luc*, luciferase; PH, partial hepatectomy.

reduced (see online supplementary figure S5A–C). Furthermore, levels of *Foxm1* and cyclin A2 and B1 mRNAs were strongly reduced in Hepa1-6 and AML12 cells upon transfection with *Fgfr4* and *Fgfr4\_2* siRNAs (see online supplementary figure S5D and data not shown).

### Fgfr signalling is essential for liver regeneration

Finally, we determined whether *Fgfr1* and *Fgfr2* prevent a more severe phenotype in *Fgfr4* knockdown mice. For this purpose, we injected *Luc* or *Fgfr4* siRNA into Alb-R1/R2 mice or Alb-Cre mice. Alb-R1/R2 mice showed impaired expression of genes required for compound detoxification, resulting in liver necrosis and an almost 50% reduction in survival upon PH when ketamine/xylazine was used for anaesthesia.<sup>10</sup> Since the extent of liver injury and the resulting mortality were much lower with isoflurane anaesthesia,<sup>10</sup> we used these conditions for our experiments. While Alb-R1/R2 mice with *Fgfr4* knockdown (Alb-R1/R2-*Fgfr4* mice) survived the first two days after PH, they subsequently showed signs of liver failure and they died or had to be sacrificed due to health problems (figure 4A). BrdU staining and expression analysis of cyclins A2 and B1 revealed strongly reduced hepatocyte proliferation in the remaining mice at 72 h, and at this time we also observed massive necrosis, liver damage and steatosis (figure 4B–E). In

addition, *Fgf15* serum levels were dramatically increased (figure 4E), indicating high levels of bile acids that reach the intestine. Indeed, levels of intrahepatic bile acids were already higher prior to PH in Alb-R1/R2-*Fgfr4* mice and dramatically increased at 72 h after PH when liver failure occurred (figure 4E and see online supplementary table S1). Thus, in contrast to mice deficient in only *Fgfr4*, levels of intrahepatic bile acids did not decrease after 48 h in Alb-R1/R2-*Fgfr4* mice, and the animals were not able to repair the necrotic damage. These results demonstrate that *Fgfr* signalling in hepatocytes is essential for liver regeneration.

### DISCUSSION

We demonstrate a severe impairment of liver regeneration upon knockdown of *Fgfr4* in hepatocytes, consistent with the important role of *Fgfr4* in liver tumorigenesis through its effect on hepatoma cell proliferation and survival.<sup>12</sup> Thus, targeting this receptor is a potential treatment option for this malignancy.<sup>13–16</sup> Surprisingly, however, mice with a global *Fgfr4* knockout exhibited no defect in hepatocyte proliferation after PH, and recovery of their liver mass was not affected.<sup>11</sup> The different results obtained with *Fgfr4* knockout versus knockdown mice may result from activation of compensatory mechanisms in the knockout mice during prenatal or postnatal development. They

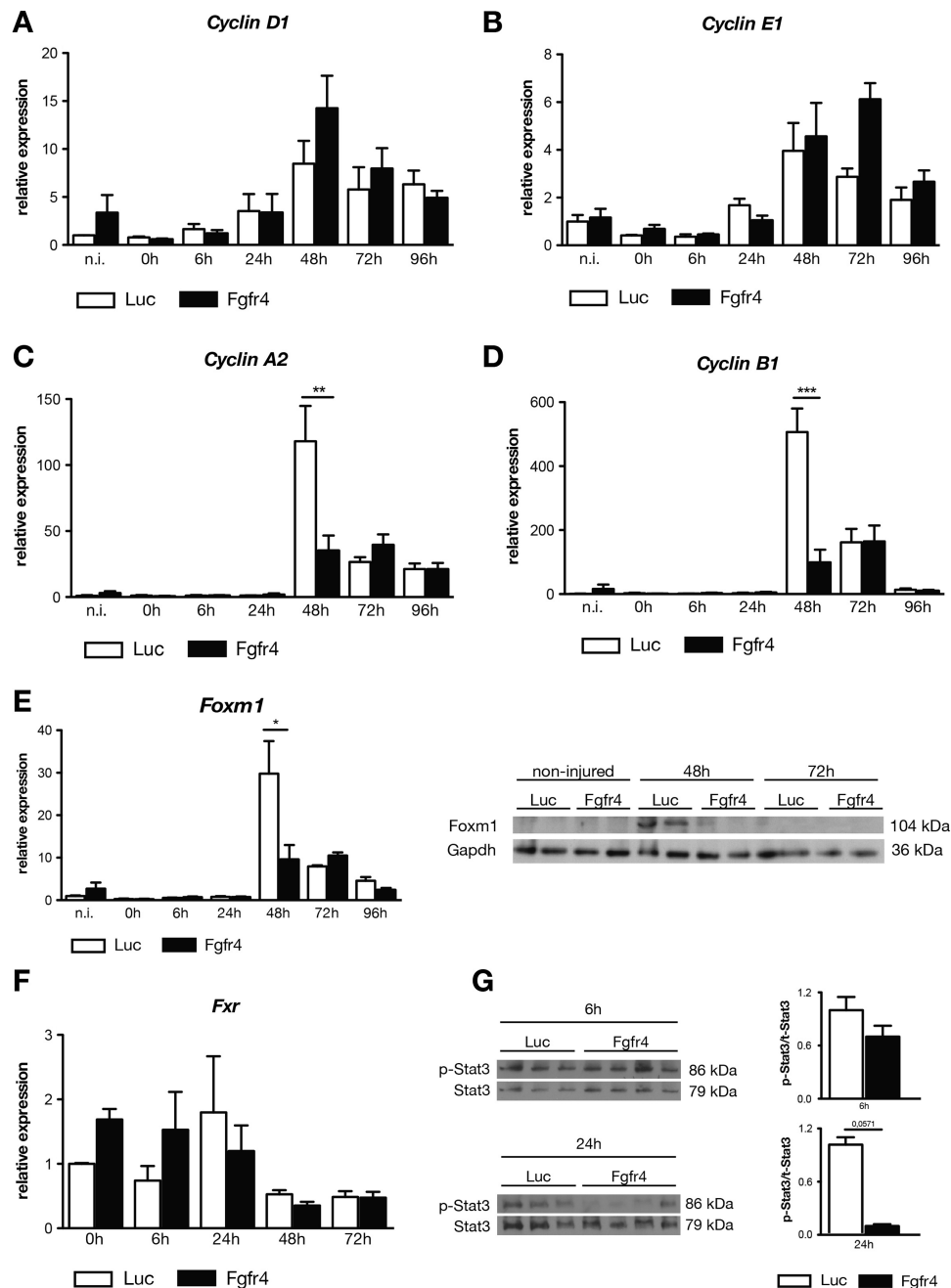


**Figure 3** Cell cycle progression is impaired in mice with *Fgfr4* knockdown. (A–F) qRT-PCR analysis of different cyclins and of *Foxm1* and *Fxr* using RNAs from liver at different time points after PH. N=3–9 per time point and treatment group. Expression levels in non-injured liver of mice injected with *Luc* siRNA were arbitrarily set as 1. (E and G) Total liver lysates of mice prior to and at different time points after PH were analysed by western blotting for expression of *Foxm1* and *Gapdh* (E), or total and phosphorylated *Stat3* (G). The ratio between phosphorylated and total *Stat3* is shown. All bars represent mean±SEM. *Fgfr*, fibroblast growth factor receptor; *Luc*, luciferase; PH, partial hepatectomy.

are unlikely caused by off-target effects of the siRNA since the same abnormalities were observed with two different *Fgfr4* siRNAs. In addition, toxicity of the nanoparticles was excluded since we did not observe liver abnormalities in mice after injection of nanoparticles with *Luc* siRNA—not even after PH. Most importantly, loss of *Fgf15* caused similar alterations in liver regeneration as seen after *Fgfr4* knockdown,<sup>27 28</sup> and loss of *Fxr* in the intestine also resulted in impaired hepatocyte proliferation after PH, which was rescued by adenoviral overexpression of *Fgf15*.<sup>29</sup> However, the strong lethality observed after PH in *Fgf15* knockout mice<sup>27</sup> was not observed in *Fgfr4* knockdown animals and we also did not find a reduction in *Fxr* or

cyclin D1 expression after *Fgfr4* knockdown. *Fgf15* can also activate the IIIc variants of *Fgfr1*, *Fgfr2* or *Fgfr3*,<sup>30</sup> which are expressed on non-parenchymal cells, and this may contribute to the effect of *Fgf15* on liver regeneration. Hepatocytes only express the IIb variants of *Fgfr1* and *Fgfr2*,<sup>10</sup> which are most likely not activated by *Fgf15*. However, we cannot fully exclude the possibility that *Fgf15* activates these receptors in hepatocytes in vivo. Finally, activation of *Fgfr4* by *Fgf15* in other organs, which are not targeted by the siRNA, may contribute to the effect of *Fgf15* on liver regeneration. However, it seems most likely that very low levels of *Fgfr4* that remain in the liver of the siRNA-treated mice are sufficient to maintain normal

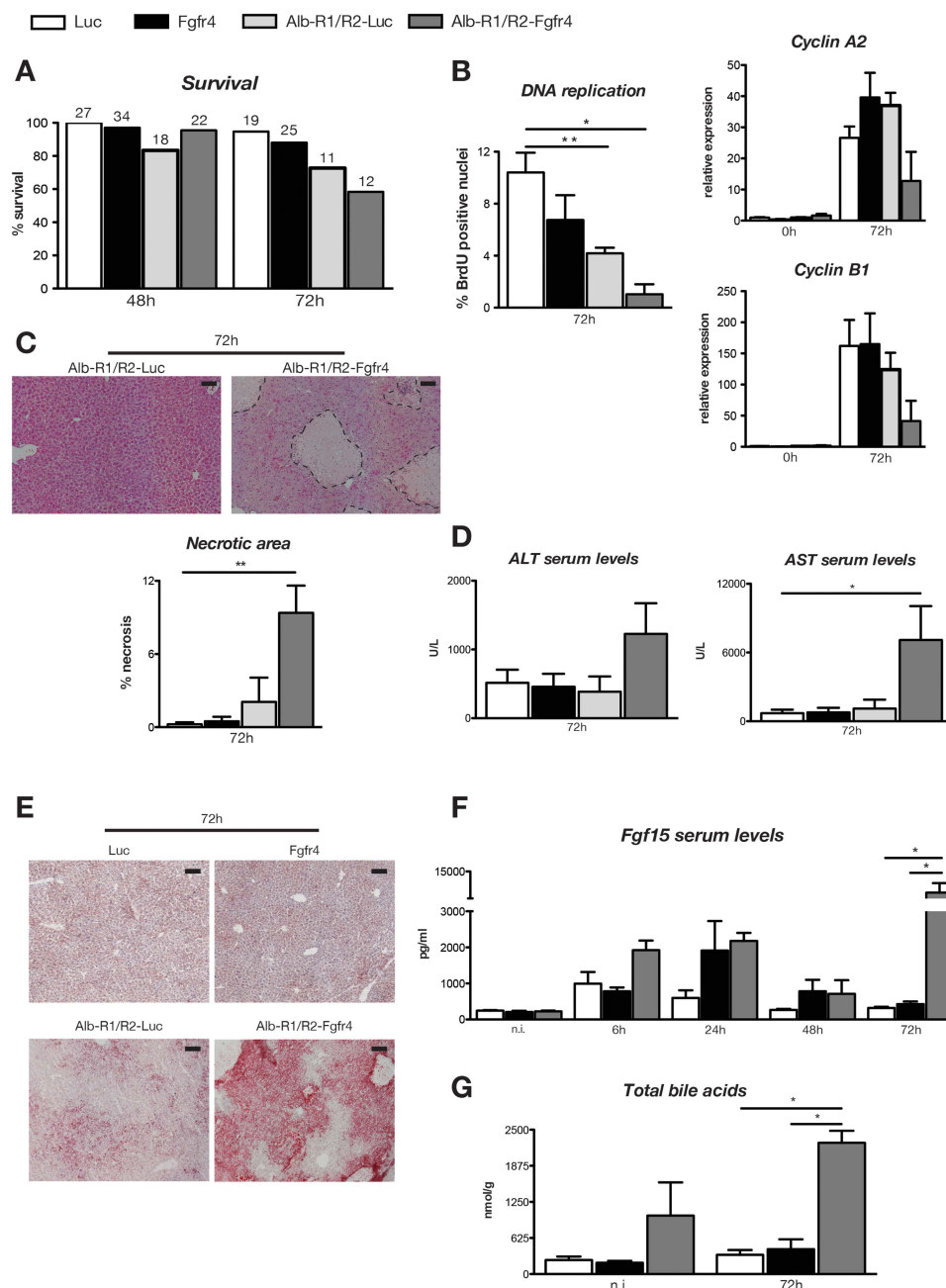


**Figure 4** Fgfr signalling is essential for liver regeneration. Alb-R1/R2 mice or Alb-Cre control mice were injected with *Fgfr4* or *Luc* siRNA and subjected to PH. Survival of mice of all genotypes and treatment groups is shown on (A). The number on top of the bars indicates the number of mice included in the analysis at each time point. (B) Left panel: BrdU-positive cells were counted in liver sections 72 h after PH in Alb-R1/R2 mice and Alb-Cre control mice injected with *Fgfr4* or *Luc* siRNA. N=4–9 per time point and treatment group. Right panels: qRT-PCR analysis of cyclins A2 and B1 using RNAs from liver at 0 h and 72 h after PH. N=3–9 per time point and treatment group. Expression levels in mice injected with *Luc* siRNA 0 h after PH were arbitrarily set as 1. N=4–9. (C) The necrotic area (encircled with dotted line) was determined in H/E-stained sections. N=4–9. (D) ALT and AST activities in the serum of mice of all treatment groups at 72 h after PH. N=4–9. (E) Hepatic steatosis as determined by Oil Red O staining of liver sections. Representative sections from 3–10 mice per treatment group are shown. (F) Serum levels of Fgf15 at different time points after PH. N=3–5. (G) Levels of total intrahepatic bile acids were determined using liquid chromatography–mass spectrometry. N=3–5. All bars represent mean±SEM. ALT, alanine transaminase; AST, aspartate transaminase; BrdU, 5-bromo-2'-deoxyuridine; Fgfr, fibroblast growth factor receptor; Luc, luciferase; PH, partial hepatectomy.

expression levels of *cyclin D1* and *Fxr* and to allow survival. Alternatively, differences in the analgesia or anaesthesia, the surgical procedure and/or the genetic background may contribute to the differences in liver regeneration between *Fgfr4* knock-down and *Fgf15* knockout mice.

Our mechanistic studies combined with published data strongly suggest that an Fgf15-Fgfr4-Stat3-Foxm1 axis controls

hepatocyte DNA replication and proliferation in the regenerating liver. This hypothesis is based on the following findings: (i) Fgf15 serum levels strongly increased after PH, (ii) loss of Fgf15 caused a similar regeneration defect as knockdown of Fgfr4, (iii) activation of Stat3 and induction of Foxm1 expression by PH were strongly reduced upon knockdown of Fgfr4 in the liver and (iv) knockdown of Fgfr4 in cultured hepatoma cells also



reduced the levels of pStat3 and concomitantly resulted in accumulation of cells in G1 and in reduction of DNA synthesis. We propose that the failure to induce Foxm1 expression after PH is primarily responsible for the impaired DNA replication in hepatocytes since Foxm1-deficient mice showed similar abnormalities and also lacked the strong peak of hepatocyte DNA replication that is normally seen 36–48 h post PH.<sup>24</sup> By contrast, these mice did not show liver necrosis, indicating that the necrosis seen after PH in *Fgfr4* knockdown mice is Foxm1 independent. In addition, it is obviously not due to major damage of the portal bile ductules. Rather, it seems most likely that the effect of *Fgfr4* on bile acid metabolism<sup>11 31</sup> underlies this phenotype. Similar as in *Fgf15*-deficient mice, this leads to accumulation of cytotoxic bile acids in the liver after PH. The enhanced expression of *Cyp7a1* in the non-injured liver of control mice compared with *Fgfr4* knockdown mice provides a partial explanation for this finding. However, the PH-induced down-regulation of *Cyp7a1* expression<sup>32</sup> was not affected in *Fgfr4* knockdown mice. This down-regulation was shown to depend on Hgf,<sup>33</sup> which was normally expressed in *Fgfr4* knockdown mice (see online supplementary figure S6A). Therefore, additional mechanisms, such as defects in the PH-induced regulation of different transporters,<sup>23 32</sup> are likely to contribute to the accumulation of bile acids in the liver, which remain to be determined. Consistent with the increase in bile acids, which stimulate expression of *Fgf15* in the intestine via activation of Fxr,<sup>21</sup> serum levels of *Fgf15* were much higher in *Fgfr4* knockdown mice compared with *Luc* siRNA-injected mice after PH.

The most dramatic result of our study was the liver failure that occurred between 48 and 72 h after PH in Alb-R1/R2-*Fgfr4* mice. This resulted from severe liver necrosis, which—in contrast to mice with loss of only *Fgfr4* or *Fgfr1/Fgfr2*—could not be repaired. The necrosis is most likely the consequence of the prolonged increase in intrahepatic bile acids after PH, which causes continuous cell damage. The molecular mechanisms underlying this strong increase are as yet unknown since *Cyp7a1* expression was not significantly altered in Alb-R1/R2-*Fgfr4* mice prior and following PH (see online supplementary figure S6B), possibly due to activation of compensatory mechanisms. Therefore, *Fgfr* deficiency seems to affect other steps in bile acid metabolism and/or transport, which should be addressed in future studies. The bile acid toxicity in combination with the repair defect ultimately resulted in liver failure. The severe lipid accumulation that we observed after PH is likely to further contribute to the severe regeneration phenotype since hepatic steatosis has been shown to affect hepatocyte proliferation after PH.<sup>34 35</sup>

Taken together, our results revealed that Fgfs and their receptors are essential orchestrators of liver regeneration. This is likely to be of major medical relevance because the remarkable capacity of the liver to regenerate is insufficient after chronic injury or upon removal of particularly large amounts of liver tissue. In the latter case, the remaining liver tissue is too small to fulfil the important functions of this organ in metabolism and detoxification, ultimately resulting in small-for-size syndrome and liver failure. Remarkably, the reduced survival that occurs after extended PH (86%) was partially rescued by adenoviral delivery of *Fgf15*.<sup>27</sup> Furthermore, inducible overexpression of *Fgf7* in transgenic mice prevented chronic liver damage and even stimulated repair after chronic injury, most likely through the activation of *Fgfr2-IIIb* on liver progenitor cells.<sup>36</sup> Thus, Fgfs are emerging as promising therapeutics for the prevention and/or treatment of liver damage and for the improvement of the regeneration process in this organ.

**Acknowledgements** We thank Dr Lucia Bautista Borrego, Dr Michael Meyer, Dr Michèle Telorack, Beat Siegenthaler, Lucia Pelloni and Christiane Born-Berclaz (ETH Zurich) for experimental help, Dr David Ornitz (Washington University St. Louis, USA) for providing conditional *Fgfr1/Fgfr2* knockout mice and for helpful suggestions, Dr Achim Weber (University of Zurich) for support, and Sol Taguinod (ETH Zurich) for help with animal care. This work was supported by the Swiss National Science Foundation (310030\_132884 to SW), a postdoctoral fellowship from the Deutsche Forschungsgemeinschaft (to TS), and a predoctoral fellowship from the Janggen-Pöhn Stiftung (to MB).

**Contributors** SP-A, MB, RLB, LP, TR, FB, GL and TS performed the experiments and analysed the data. CH was involved in the bile acid analysis, VK coordinated the siRNA research, SW wrote the manuscript and designed the project together with SP-A. DMO provided conditional *Fgfr1/Fgfr2* knockout mice. Achim Weber supported the work of Friederike Böhm. Lucia Bautista Borrego, Michael Meyer, Michele Telorack, Lucia Pelloni and Beat Siegenthaler helped with some of the experiments.

**Competing interests** None.

**Provenance and peer review** Not commissioned; externally peer reviewed.

## REFERENCES

- 1 Itoh N, Ornitz DM. Evolution of the Fgf and Fgfr gene families. *Trends Genet* 2004;20:563–9.
- 2 Beenken A, Mohammadi M. The FGF family: biology, pathophysiology and therapy. *Nat Rev Drug Disc* 2009;8:235–53.
- 3 Werner S, Peters KG, Longaker MT, et al. Large induction of keratinocyte growth factor expression in the dermis during wound healing. *Proc Natl Acad Sci USA* 1992;89:6896–900.
- 4 Werner S, Smola H, Liao X, et al. The function of KGF in morphogenesis of epithelium and reepithelialization of wounds. *Science* 1994;266:819–22.
- 5 Braun S, auf dem Keller U, Steiling H, et al. Fibroblast growth factors in epithelial repair and cytoprotection. *Philos Trans R Soc London Biol Sci* 2004;359:753–7.
- 6 Fausto N. Liver regeneration. *J Hepatol* 2000;32:19–31.
- 7 Michalopoulos GK. Liver regeneration. *J Cell Physiol* 2007;213:286–300.
- 8 Böhm F, Kohler UA, Speicher T, et al. Regulation of liver regeneration by growth factors and cytokines. *EMBO Mol Med* 2010;2:294–305.
- 9 Steiling H, Wustefeld T, Bugnon P, et al. Fibroblast growth factor receptor signalling is crucial for liver homeostasis and regeneration. *Oncogene* 2003;22:4380–8.
- 10 Böhm F, Speicher T, Hellerbrand C, et al. FGF receptors 1 and 2 control chemically induced injury and compound detoxification in regenerating livers of mice. *Gastroenterology* 2010;139:1385–96.
- 11 Yu C, Wang F, Kan M, et al. Elevated cholesterol metabolism and bile acid synthesis in mice lacking membrane tyrosine kinase receptor FGFR4. *J Biol Chem* 2000;275:15482–9.
- 12 Ho HK, Pok S, Streit S, et al. Fibroblast growth factor receptor 4 regulates proliferation, anti-apoptosis and alpha-fetoprotein secretion during hepatocellular carcinoma progression and represents a potential target for therapeutic intervention. *J Hepatol* 2009;50:118–27.
- 13 Mellor HR. Targeted inhibition of the FGF19-FGFR4 pathway in hepatocellular carcinoma; translational safety considerations. *Liver Int* 2014;34:e1–9.
- 14 Love KT, Mahon KP, Levins CG, et al. Lipid-like materials for low-dose, in vivo gene silencing. *Proc Natl Acad Sci USA* 2010;107:1864–9.
- 15 Akinc A, Querbes W, De S, et al. Targeted delivery of RNAi therapeutics with endogenous and exogenous ligand-based mechanisms. *Mol Ther* 2010;18:1357–64.
- 16 Jayaraman M, Ansell SM, Mui BL, et al. Maximizing the potency of siRNA lipid nanoparticles for hepatic gene silencing in vivo. *Angewandte Chemie* 2012;51:8529–33.
- 17 Zeigerer A, Gilleron J, Bogorad RL, et al. Rab5 is necessary for the biogenesis of the endolysosomal system in vivo. *Nature* 2012;485:465–70.
- 18 Speicher T, Siegenthaler B, Bogorad RL, et al. Loss of  $\beta$ 1-integrin in hepatocytes impairs liver regeneration through inhibition of growth factor signalling. *Nat Commun* 2014;5:3862.
- 19 Muhlbauer M, Fleck M, Schutz C, et al. PD-L1 is induced in hepatocytes by viral infection and by interferon-alpha and -gamma and mediates T cell apoptosis. *J Hepatol* 2006;45:520–8.
- 20 Scherer M, Gnewuch C, Schmitz G, et al. Rapid quantification of bile acids and their conjugates in serum by liquid chromatography-tandem mass spectrometry. *J Chromatography* 2009;877:3920–5.
- 21 Inagaki T, Choi M, Moschetta A, et al. Fibroblast growth factor 15 functions as an enterohepatic signal to regulate bile acid homeostasis. *Cell Metab* 2005;2:217–25.
- 22 Chiang JY. Regulation of bile acid synthesis. *Front Biosci* 1998;3:d176–93.
- 23 Csanky IL, Aleksunes LM, Tanaka Y, et al. Role of hepatic transporters in prevention of bile acid toxicity after partial hepatectomy in mice. *Am J Physiol Gastroenterol Liver Physiol* 2009;297:G419–33.
- 24 Wang X, Kiyokawa H, Dennewitz MB, et al. The Forkhead Box m1b transcription factor is essential for hepatocyte DNA replication and mitosis during mouse liver regeneration. *Proc Natl Acad Sci USA* 2002;99:16881–6.

- 25 Mencalha AL, Binato R, Ferreira GM, *et al.* Forkhead box M1 (FoxM1) gene is a new STAT3 transcriptional factor target and is essential for proliferation, survival and DNA repair of K562 cell line. *PLoS ONE* 2012;7:e48160.
- 26 French DM, Lin BC, Wang M, *et al.* Targeting FGFR4 inhibits hepatocellular carcinoma in preclinical mouse models. *PLoS ONE* 2012;7:e36713.
- 27 Uriarte I, Fernandez-Barrena MG, Monte MJ, *et al.* Identification of fibroblast growth factor 15 as a novel mediator of liver regeneration and its application in the prevention of post-resection liver failure in mice. *Gut* 2013;62:899–910.
- 28 Kong B, Huang J, Zhu Y, *et al.* Fibroblast growth factor 15 deficiency impairs liver regeneration in mice. *Am J Physiol Gastroenterol Liver Physiol* 2014;15:G839–902.
- 29 Zhang L, Wang YD, Chen WD, *et al.* Promotion of liver regeneration/repair by farnesoid X receptor in both liver and intestine in mice. *Hepatology* 2012;56:2336–43.
- 30 Wu X, Ge H, Lemon B, *et al.* FGF19-induced hepatocyte proliferation is mediated through FGFR4 activation. *J Biol Chem* 2010;285:5165–70.
- 31 Holt JA, Luo G, Billin AN, *et al.* Definition of a novel growth factor-dependent signal cascade for the suppression of bile acid biosynthesis. *Genes Dev* 2003;17:1581–91.
- 32 Huang W, Ma K, Zhang J, *et al.* Nuclear receptor-dependent bile acid signaling is required for normal liver regeneration. *Science* 2006;312:233–6.
- 33 Zhang L, Huang X, Meng Z, *et al.* Significance and mechanism of CYP7a1 gene regulation during the acute phase of liver regeneration. *Mol Endocrinol* 2009;23:137–45.
- 34 Yang SQ, Lin HZ, Mandal AK, *et al.* Disrupted signaling and inhibited regeneration in obese mice with fatty livers: implications for nonalcoholic fatty liver disease pathophysiology. *Hepatology* 2001;34:694–706.
- 35 Selzner M, Clavien PA. Failure of regeneration of the steatotic rat liver: disruption at two different levels in the regeneration pathway. *Hepatology* 2000;31:35–42.
- 36 Takase HM, Itoh T, Ino S, *et al.* FGF7 is a functional niche signal required for stimulation of adult liver progenitor cells that support liver regeneration. *Genes Dev* 2013;27:169–81.



# Control of hepatocyte proliferation and survival by Fgf receptors is essential for liver regeneration in mice

Susagna Padrissa-Altés, Marc Bachofner, Roman L Bogorad, Lea Pohlmeier, Thomas Rossolini, Friederike Böhm, Gerhard Liebisch, Claus Hellerbrand, Victor Koteliensky, Tobias Speicher and Sabine Werner

*Gut* 2015 64: 1444-1453 originally published online November 21, 2014  
doi: 10.1136/gutjnl-2014-307874

---

Updated information and services can be found at:  
<http://gut.bmj.com/content/64/9/1444>

---

*These include:*

**Supplementary  
Material**

Supplementary material can be found at:  
<http://gut.bmj.com/content/suppl/2014/11/21/gutjnl-2014-307874.DC1>

**References**

This article cites 36 articles, 11 of which you can access for free at:  
<http://gut.bmj.com/content/64/9/1444#BIBL>

**Email alerting  
service**

Receive free email alerts when new articles cite this article. Sign up in the box at the top right corner of the online article.

---

**Notes**

---

To request permissions go to:  
<http://group.bmj.com/group/rights-licensing/permissions>

To order reprints go to:  
<http://journals.bmj.com/cgi/reprintform>

To subscribe to BMJ go to:  
<http://group.bmj.com/subscribe/>